Journal of Physiology (1992), **450**, *pp.* 529–546
With 10 *figures*
Printed in Great Britain

TETRODOTOXIN-SENSITIVE CALCIUM-CONDUCTING CHANNELS IN THE RAT HIPPOCAMPAL CA1 REGION

BY NORIO AKAIKE AND KAZUYOSHI TAKAHASHI

From the Department of Neurophysiology, Tohoku University School of Medicine, Sendai 980, Japan

(*Received 1 October 1991*)

SUMMARY

1. Tetrodotoxin (TTX)-sensitive Ca^{2+} conducting channels which produce a transient inward current were investigated in pyramidal neurones freshly dissociated from the dorsal part of rat hippocampal CA1 region by the use of the suction-pipette technique, which allows for intracellular perfusion under a single-electrode voltage clamp.

2. In all cells superfused with Na^+- and K^+-free external solution containing 10 mM-Ca^{2+} and 10^{-5} M-La^{3+}, a transient inward Ca^{2+} current was evoked by a step depolarization to potentials more positive than about −50 mV from a holding potential (V_H) of −100 mV. This current was inhibited by either removing the extracellular Ca^{2+} or adding TTX (termed as 'TTX-I_{Ca}').

3. Activation and inactivation processes of the TTX-I_{Ca} were highly potential dependent at 20–22 °C, and the latter was fitted by a double exponential function. The time to peak of the current decreased from 5·0 to 2·3 ms at a test potential change from −50 to 0 mV. The time constants of the current decay decreased from 2·8 to 2·2 ms for fast component (τ_{if}) and from 16·0 to 8·2 ms for slow component (τ_{is}) at a potential change from −35 to −10 mV.

4. The TTX-I_{Ca} was activated at threshold potential of about −55 mV and reached full activation at −30 mV. The steady-state inactivation of TTX-I_{Ca} could be fitted by a Boltzmann equation with a slope factor of 6·0 mV and a half-inactivation voltage of −72·5 mV.

5. Biphasic recovery (reactivation) from the complete inactivation of TTX-I_{Ca} was observed. The time constant of the major component (78·8 to 91·6 % of total) of the reactivation was 13·1 ms, and that of the minor one was 120 to 240 ms. Therefore, TTX-I_{Ca} remained fairly constant at a train of stimulation up to 3 Hz. However, the inhibition of current amplitude occurred as the repetitive stimulation increased more than 10 Hz, and considerable tonic inhibition occurred with increasing stimulation frequency.

6. When the peak amplitudes in the individual current–voltage (I–V) relationships of TTX-I_{Ca} at various extracellular Ca^{2+} concentrations ($[Ca^{2+}]_o$) were plotted as a function of $[Ca^{2+}]_o$, the current amplitude increased linearly without showing any saturation.

7. The ratio of peak amplitude in the individual I–V relationships of Ca^{2+}, Sr^{2+} and

Ba^{2+} currents passing through the TTX-sensitive Ca^{2+} conducting channel was 1:0·33:0·05, although the current kinetics were much the same.

8. Adding Na^+ to an external solution containing 5 mM-Ca^{2+} and 10^{-5} M-La^{3+} elicited the current consisting of two components: one had a rapid inactivation and another a slow inactivation. The inactivation kinetics of fast and slow current components were the same as those of Na^+ current (I_{Na}) and TTX-I_{Ca}, respectively. The current amplitude of the slow component increased with increasing the extracellular Na^+ concentration ($[Na^+]_o$).

9. TTX inhibited the TTX-I_{Ca} in a time- and concentration-dependent manner without affecting the current kinetics. The time course for steady-state inhibition shortened in minutes with increasing concentration. Lignocaine inhibited the TTX-I_{Ca} within a second in a concentration-dependent manner, with accelerating the inactivation process. The concentrations of half-inhibition (IC_{50}) were $3·5 \times 10^{-9}$ M for TTX and $3·6 \times 10^{-4}$ M for lignocaine.

10. Scorpion toxin prolonged the inactivation phase of TTX-I_{Ca} in a time- and concentration-dependent manner. In the toxin-treated neurones, both the time constant of τ_{is} and its functional contribution to the total current increased with increasing the toxin concentration.

11. It was concluded that the TTX-I_{Ca} is carried by Ca^{2+} and that Na^+ can pass through this TTX-sensitive Ca^{2+} conducting channels. The physiological and pharmacological properties of the TTX-sensitive Ca^{2+} conducting channels were also compared with those of voltage-dependent Na^+ channels and low-threshold (T-type) Ca^{2+} channels.

INTRODUCTION

In the squid giant axon the Ca^{2+} influx through the voltage-dependent Na^+ channels has been shown with radioactive Ca^{2+} (Hodgkin & Keynes, 1957; Tasaki, Watanabe & Lerman, 1967). With aequorin as Ca^{2+} indicator, two types of Ca^{2+} influxes were observed in the squid axon during the membrane depolarization: one is tetrodotoxin (TTX)-sensitive and the other TTX-insensitive (Barker, Hodgkin & Ridgway, 1971). According to Watanabe, Tasaki, Singer & Lerman (1967), action potentials from squid axon perfused with 25 mM-CsF glycerol as internal solution and with 100 or 200 mM-$CaCl_2$ plus glycerol as external solution were blocked by TTX, indicating that at least part of the inward current is going through the Na^+ channels. Voltage-clamp experiments carried out on the same preparation clearly showed that there is a TTX-sensitive Ca^{2+} inward current (I_{Ca}) which is different from the time course of the voltage-dependent Na^+ inward current (I_{Na}) (Meves & Vogel, 1973). Okamoto, Takahashi & Yoshii (1976) reported that the I_{Ca} is tunicate egg cell superfused with Na^+-free artificial sea water containing Ca^{2+} are separated into two current components. One component is similar to the I_{Ca} in common excitable cell membranes, and the other component is the one flowing through the egg Na^+ channels, although the current is insensitive to TTX (Okamoto, Takahashi & Yoshii, 1975). Sorbera & Morad (1990) have reported that atrionatriuretic peptide (ANP) converts mammalian cardiac Na^+ channels to a Ca^{2+} conducting form.

Recently, we found that the pyramidal neurones acutely dissociated from rat hippocampal CA1 region also have TTX-sensitive Ca^{2+} conducting channels which

induce a transient Ca^{2+} inward current (termed as 'TTX-I_{Ca}') (Takahashi, Wakamori & Akaike, 1989). Interestingly, the TTX-sensitive Ca^{2+} conducting channels were found in the neurones located dominantly at the dorsal portion of the hippocampal CA1 region, indicating heterogeneous distribution of TTX-sensitive Ca^{2+} conducting channels (Akaike, Takahashi & Morimoto, 1991). In the present experiments, therefore we have investigated the current kinetics and pharmacological properties of the TTX-sensitive Ca^{2+} conducting channels in comparison with those of voltage-dependent Na^+ channels and T-type Ca^{2+} channels which also induce transient inward currents. The physiological roles of TTX-I_{Ca} are also discussed.

METHODS

Preparation. Single pyramidal neurones of hippocampal CA1 region were dissociated from 10- to 15-day-old rats as reported previously (Kaneda, Nakamura & Akaike, 1988; Akaike, Kostyuk & Osipchuk, 1989). In brief, the brain was removed from rats anaesthetized with ether and dissected into slices (500 μm thick), using a microslicer (D.S.K., DTK-1000). The whole brain slices containing the hippocampal CA1 region were selected and recovered in an incubation solution bubbled for 50 min at 31 °C with 95% O_2 plus 5% CO_2. After the pre-incubation the slices were treated enzymatically in an incubation solution containing 1 mg/ml collagenase and 1 mg/ml trypsin, in which they were kept for 40 min at 31 °C. After the enzyme treatments, the slices were washed at least three times with Ca^{2+}-free EGTA incubation solution. Since the TTX-sensitive Ca^{2+} conducting channels and T-type Ca^{2+} channels are distributed heterogeneously in the pyramidal neurones of the dorsal and ventral parts of rat hippocampal CA1 regions, respectively (Akaike *et al.* 1991), the experiments for recording TTX-I_{Ca} were made on pyramidal neurones dissociated freshly from the dorsal part of CA1 region whereas the measurements of both T-type I_{Ca} and I_{Na} were performed on pyramidal neurones from the ventral part. The individual parts were removed by micro-punching and dispersed mechanically by pipetting. Dissociated pyramidal neurones were kept in a normal external solution (Table 1) containing 1% bovine serum at room temperature (20–22 °C). They were viable for electrophysiological studies for up to 12 to 15 h.

Cell perfusion. Selected neurones were transferred into a culture dish (Cornig, 35 mm) and drawn into the opening of a glass pipette (1·5 to 2 μm in diameter) filled with the internal solution. The resistance of electrodes filled with internal solution was 2–5 MΩ. The membrane patch in the opening was destroyed by negative pressure, and soluble cell contents were exchanged with the internal (pipette-filling) solution by diffusion (Akaike *et al.* 1989).

Electrical measurements. A suction-pipette technique was applied to the dissociated hippocampal pyramidal neurones (Akaike *et al.* 1989). Handling of neurones under the microscope was done by the use of a water-drive micro-manipulator (Narishige, MW-3). Recording electrodes for suction-pipette technique were pulled on a two stage puller (Narishige, PB-7) and fire-polished on a microforge (Narishige, MF-83). Transmembrane currents were recorded using a patch-clamp amplifier (Nihon Kohden, CEZ-2300), and both current and voltage were monitored on a storage oscilloscope (Toshiba, 10M63). Simultaneously, the data were stored on FM tape (TEAC, MR-30) at a digitizing rate of 5 kHz for computer analysis using pCLAMP (Axon Instruments). The current signal was filtered at 3 kHz (NF Electronic Instruments, FV-655) before sampling at 0·33 ms per point. The cells had a mean input resistance of $2·8 \pm 0·5$ GΩ ($n = 36$). The amplitude of current was measured at the peak of each current. Since no rectification was elicited by large hyperpolarizing step pulses, the linear components of transient capacitative and leakage currents associated with the ionic currents in most of the experiments were subtracted by adding the current response to equal but opposite voltage steps using a signal averager (Nihon Kohden, ATAC-150).

Rapid application of external test solutions. An extremely rapid concentration jump termed 'concentration-clamp' technique was used (Akaike, Inoue & Krishtal, 1986). The cell-attached tip of a suction electrode was inserted into a polyethylene tube through a circular hole of approximately 500 μm in diameter. The lower end of this tube could be submerged in external solution contained in plastic dishes on a turntable. A negative pressure (-35 cmH_2O) applied to the upper end of the polyethylene tube was controlled by an electromagnetic valve driven by 24 V

DC. The power supply was switched on for the desired durations by a pulse generator (Nihon Kohden, SEN-7103). The solution exchange around the dissociated hippocampal pyramidal neurones was completed within 1 to 2 ms.

Solutions. The ionic compositions of external test solutions used are listed in Table 1. The internal solution used for TTX-I_{Ca} and T-type I_{Ca} recordings was (mM): *N*-methyl-D-glucamine fluoride (NMG-F) 100, TEA-Cl 20 and HEPES 10. The internal solution for recording I_{Na} contained

TABLE 1. Ionic composition of external solution (ES) in mM concentration

	Incubation solution	Ca^{2+}-free EGTA	Normal ES	TTX-I_{Ca} ES	I_{Na} ES	T-type I_{Ca} ES
NaCl	124	124	150	—	20	—
Choline chloride	—	—	—	140	136	140
KCl	5	5	5	—	—	—
CsCl	—	—	—	5	5	5
KH_2PO_4	1·2	1·2	—	—	—	—
$CaCl_2$	2·4	—	2	10	2	10
$MgCl_2$	—	—	1	—	—	—
$MgSO_4$	1·3	1·3	—	—	—	—
$NaHCO_3$	26	26	—	—	—	—
Glucose	10	10	10	10	10	10
EGTA	—	2	—	—	—	—
HEPES	—	—	10	10	10	10
$LaCl_3$	—	—	—	10^{-5} M	10^{-5} M	—
TTX	—	—	—	—	—	10^{-7} M
pH	7·4[A]	7·4[A]	7·4[B]	7·4[B]	7·4[B]	7·4[B]

The pH was adjusted by bubbling with 95% O_2+5% CO_2 (A) and by adding Tris-base (B).

15 mM-Na^+, in which 15 mM-NMG-F was replaced with equimolar NaF. The pH of these internal solutions was adjusted to 7·2 by adding an appropriate amount of tris(hydroxymethyl)aminomethane (Tris-base). All experiments were carried out at room temperature (20–22 °C).

Drugs. Drugs used in the experiment were: collagenase type I, lignocaine, scorpion toxin *Leiurus Quinquestriatus* and ethyleneglycol-bis-(β-aminoethylether)-*N,N'*-tetracetic acid (EGTA) (Sigma), 4-(2-hydroxyethyl)-1-piperazineethanesulphonic acid (HEPES) (Dojin), trypsin and tetrodotoxin (TTX) (Sankyo). They were dissolved in the test solutions just before use. Values are expressed as means ± standard error (S.E.M.) of the mean, and significance was tested by Student's *t* test.

RESULTS

Potential- and time-dependent characteristics of TTX-sensitive I_{Ca}

The pyramidal neurones dissociated from the dorsal part of the hippocampal CA1 region were superfused with Na^+-free external solution containing 10 mM-Ca^{2+} and 10^{-5} M-La^{3+}, at which concentration La^{3+} completely blocks all voltage-dependent T-, N- and L-type I_{Ca}s (Fox, Nowycky & Tsien, 1987; Takahashi *et al.* 1989), and with Na^+-free internal solution. The TTX-I_{Ca} was induced by a 60 ms depolarization to about −60 mV from a holding potential (V_h) of −100 mV. The right panel of Fig. 1*A* shows typical TTX-I_{Ca}s in one neurone stimulated by various depolarizing pulses. In Fig. 1*B*, the current–voltage (*I–V*) relationship for TTX-I_{Ca} is plotted for the peak amplitude of individual currents, in which the maximum peak inward current appeared at about −30 mV in the *I–V* relationship. Figure 1*C* shows the *I–V* relationship for TTX-I_{Ca} after the subtraction of non-specific outward current (I_{NS}), shown by the symbol (□) in Fig. 1*B*. The TTX-I_{Ca} did not reverse even at depolarizing pulses over +10 mV (Fig. 1*B*). Figure 1*A* (left panel) and *C* show the

voltage-dependent Na^+ current (I_{Na}) in a neurone perfused with external solution containing 20 mM-Na^+, 2 mM-Ca^{2+} and 10^{-5} M-La^{3+} and with internal solution containing 15 mM-Na^+. It is evident in these figures that the kinetic characteristics of TTX-I_{Ca} are very close to those of I_{Na}.

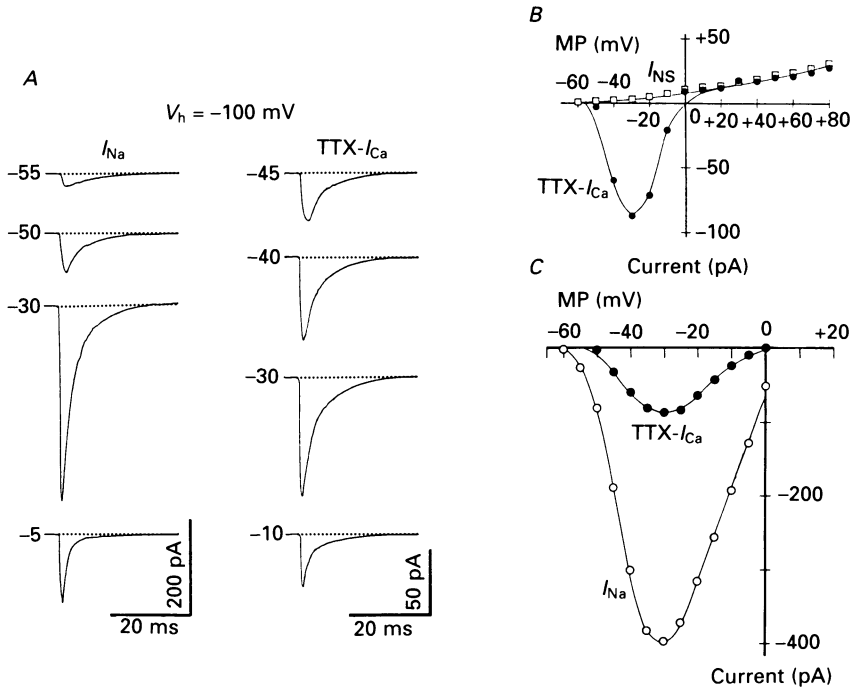

Fig. 1. The voltage-dependent Na^+ current (I_{Na}) and tetrodotoxin-sensitive Ca^{2+} current (TTX-I_{Ca}) in the pyramidal neurones dissociated from the ventral and dorsal parts of rat hippocampal CA1 region, respectively. The I_{Na} was recorded in neurones superfused with external solution containing 20 mM-Na^+, 2 mM-Ca^{2+} and 10^{-5} M-La^{3+} and internal solution containing 15 mM-Na^+. The TTX-I_{Ca} was recorded from neurones in Na^+-free external solution containing 10 mM-Ca^{2+} and 10^{-5} M-La^{3+}, and Na^+-free internal solution. *A*, typical example of I_{Na} and TTX-I_{Ca} at testing potentials having a duration of 60 ms. Holding potential (V_h) was −100 mV. Sample records of these currents were obtained after subtraction of leakage and capacitative currents. *B*, the current–voltage (*I–V*) relationship for TTX-I_{Ca} (●) and I_{NS} (□) shows the non-specific outward current. Reversal current of TTX-I_{Ca} was not observed. *C*, *I–V* relationships for TTX-I_{Ca} and I_{Na} were obtained after the subtraction of I_{NS} for the respective *I–V* relationships.

The kinetic properties of TTX-I_{Ca} were analysed by measuring the activation time (time to peak) and the inactivation time (decay time constant), at different membrane potentials. Figure 2*B* illustrates the representative TTX-I_{Ca} recording used for the kinetic analysis. In the figure, the current decay could be fitted by the sum of two components. In Fig. 2*A* and *C* the time to peak (t_p) and the fast and slow decay time constants (τ_{if} and τ_{is}, respectively) of TTX-I_{Ca} are plotted against the membrane potential (MP in millivolts). As can be seen, both the activation and inactivation of the TTX-I_{Ca} are potential dependent, the responses becoming more rapid with increasing depolarization.

Figure 2*A* also shows the t_p of both low-threshold (T-type) I_{Ca} and I_{Na} plotted against the membrane potential. In this experiment, T-type I_{Ca} was recorded in neurones dissociated from the ventral part of the CA1 region. T-type I_{Ca} could be induced by a 300 ms step depolarization to various membrane potentials from a V_h

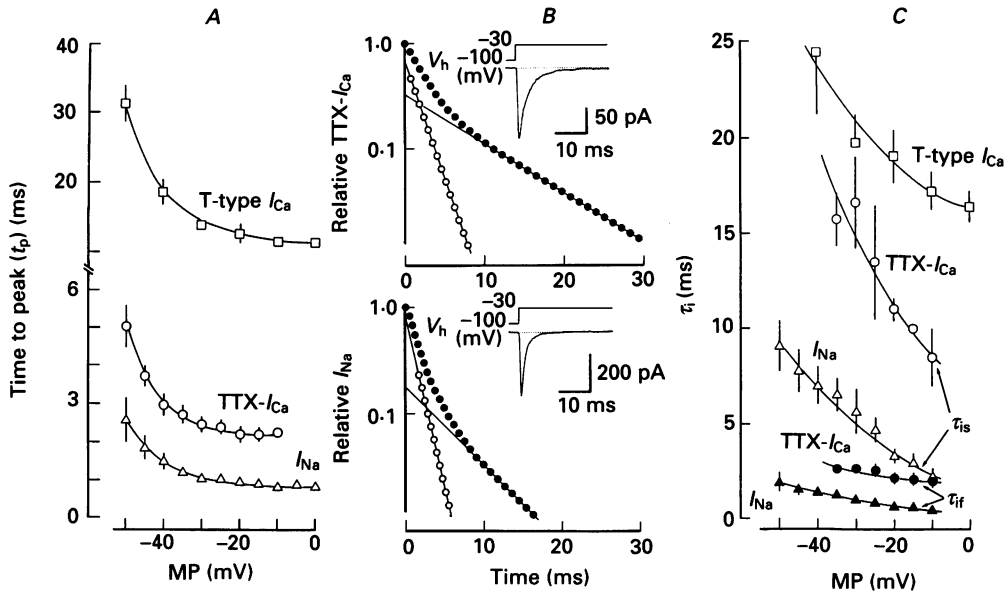

Fig. 2. Comparison of the kinetics among TTX-I_{Ca}, I_{Na} and T-type I_{Ca} in dissociated rat hippocampal pyramidal cells. Neurones were dissociated from the dorsal part for TTX-I_{Ca} recording and from the ventral part for both I_{Na} and T-type I_{Ca} recordings (Akaike *et al.* 1991). The T-type I_{Ca} was measured in Na^+-free external solution containing 10 mM-Ca^{2+} and 10^{-7} M TTX, at which concentration the TTX completely suppressed both the TTX-I_{Ca} and I_{Na} (Takahashi *et al.* 1989). *A*, voltage dependence of activation time of TTX-I_{Ca} (○), I_{Na} (△) and T-type I_{Ca} (□). The activation time was measured as the time to peak (t_p). Mean values ± S.E.M. from measurements on five neurones. In all cases V_h was −100 mV. MP, membrane potential. *B*, upper and lower panels show a typical example of TTX-I_{Ca} and I_{Na} induced by 100 and 50 ms depolarizing pulses to −30 mV from a V_h of −100 mV, respectively. Both TTX-I_{Ca} and I_{Na} decayed with a double exponence (fast and slow time constants, τ_{if} and τ_{is}, respectively). The T-type I_{Ca} showed a single exponential decay (Akaike *et al.* 1989; Takahashi & Akaike, 1991). The pulse duration for recording T-type I_{Ca} was 300 ms. *C*, voltage dependence of inactivation of TTX-I_{Ca}, I_{Na} and T-type I_{Ca}. The inactivation velocity was measured as the time constant of the exponential current decay (τ_i).

of −100 mV in Na^+-free external solution containing 10 mM-Ca^{2+} and 10^{-7} M-TTX. A semilogarithmic plot of the inactivation phase of I_{Na} also showed a double exponent (Fig. 2*B*, lower panel) whereas T-type I_{Ca} decayed with a single exponent (not shown). The results are summarized in Fig. 2*C*, in which the fast and slow time constants (τ_{if} and τ_{is} respectively) of TTX-I_{Ca} are about three times larger than those of I_{Na} at the potential range between −50 and −10 mV, but smaller than the time constant of T-type I_{Ca}. Both t_p and τ_i of all three currents were strongly potential dependent (Fig. 2*A*).

The activation curves for the TTX-I_{Ca} and I_{Na} are shown in Fig. 3*A*. The degree

of activation of both TTX-sensitive Ca^{2+} conducting channels and voltage-dependent Na^+ channels was evaluated in the following manner. The relative conductances (G_Xs) for Ca^{2+} and Na^+ (G_{Ca} and G_{Na}, respectively) normalized to the maximum ones were plotted as functions of the clamp potential (V_C) shown in Fig. 1*C*. Both the G_{Ca}

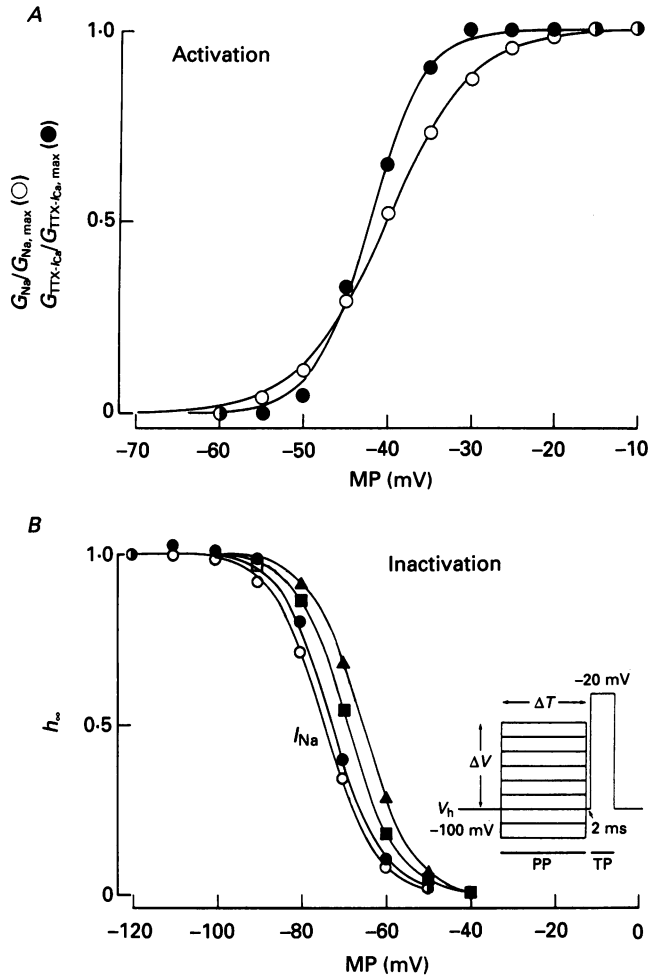

Fig. 3. Activation (*A*) and steady-state inactivation (*B*) curves for TTX-I_{Ca} and I_{Na}. Continuous curves of activation and steady-state inactivation curves were fitted by the Boltzmann equation by the use of least-squares method. Inactivation was induced by 0·1 (▲), 1 (■) and 10 (●) s prepulses for TTX-I_{Ca} and 10 s (○) prepulse for I_{Na} just before testing depolarization to −20 mV from a V_h of −100 mV (see inset). Four representative experiments were obtained.

and G_{Na} corresponded to the peak TTX-I_{Ca} and I_{Na} evoked at each V_C in the *I–V* curves respectively, and were calculated from the equation, $G_X = I_X/(V_C - E_X)$, assuming that the ionic currents, I_Xs (TTX-I_{Ca} and I_{Na}) are proportional to the driving force ($V_C - E_X$) and the zero-current potentials correspond to the equilibrium potentials, E_Xs (E_{Ca} and E_{Na}). The E_{Ca} of +60 mV was provided from our previous

report on the T-type I_{Ca} in the same preparation (Takahashi, Ueno & Akaike, 1991) since the zero-current voltage of the TTX-I_{Ca} in the present study was unclear even though the same external Ca^{2+} concentration of 10 mM was used in both studies. The E_{Na} of +7 mV was estimated from the present I–V curve (Fig. 1C) in the external

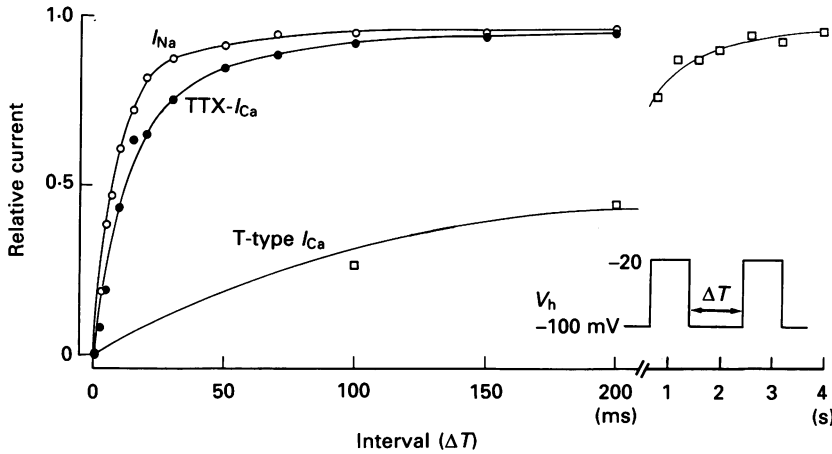

Fig. 4. Recovery from the complete inactivation of TTX-I_{Ca} (●), I_{Na} (○) and T-type I_{Ca} (□). A testing depolarizing pulses applied at different interval (ΔT) after the end of a membrane depolarization of 100 ms for TTX-I_{Ca}, 50 ms for I_{Na} and 400 ms for T-type I_{Ca}. V_h in all cases was −100 mV. Each point is the average value of four to five neurones.

and internal solutions containing 20 and 15 mM-Na^+, respectively. Results in Fig. 3A revealed that the threshold V_Cs for TTX-I_{Ca} and I_{Na} activation were −55 and −60 mV, respectively. The full activations (the maximum G_X) of TTX-I_{Ca} and I_{Na} were achieved at −30 and −20 mV, respectively. The half-maximum activation V_Cs were −42·5 mV for I_{Ca} and −40 mV for I_{Na}, and the slope factors of 3 mV for TTX-I_{Ca} and 5 mV for I_{Na} were obtained from continuous curves fitted by the Boltzmann equation.

The steady-state inactivation (h_∞) curve of TTX-I_{Ca} was measured using a conventional double pulse method (see Fig. 3B, inset) with a 0·1, 1 and 10 s prepulse to various potentials from −120 to −40 mV at a V_h of −100 mV. The relationship between h_∞ and prepulse potential was also fitted by the Boltzmann equation.

$$h(V_m) = 1/\{1+\exp[(V_m - V_{0.5})/k]\},$$

where V_m is the prepulse membrane potential, $V_{0.5}$ is the mid-potential, and k is the slope factor of 6·0 mV in the curve. When the duration of the prepulse was 0·1 s, the TTX-I_{Ca} was completely suppressed at a prepulse potential of −40 mV. When the duration of the prepulse was prolonged, the curves shifted towards the left. The estimated $V_{0.5}$ values were −65·5, −69·0 and −72·5 mV at the prepulse durations of 0·1, 1 and 10 s, respectively (Fig. 3B). The $V_{0.5}$ value was little changed by further prolongation of the prepulse beyond 10 s.

The activation and h curves of both I_{Na} and T-type I_{Ca} were also similar to those of TTX-I_{Ca}; i.e., the threshold membrane potentials in the activation curves were −60 mV for I_{Na} and −60 mV for T-type I_{Ca} whereas the $V_{0.5}$ values of h_∞–V_m curves

were −74·5 mV for I_{Na} (Fig. 3*B*) and −79 mV for T-type I_{Ca} at a prepulse duration of 10 s (Fig. 3. of Takahashi *et al.* 1991).

Figure 4 shows the time courses of recovery (reactivation) from the complete inactivation of TTX-I_{Ca}, I_{Na}, and T-type I_{Ca} at a V_h of −100 mV, measured by a

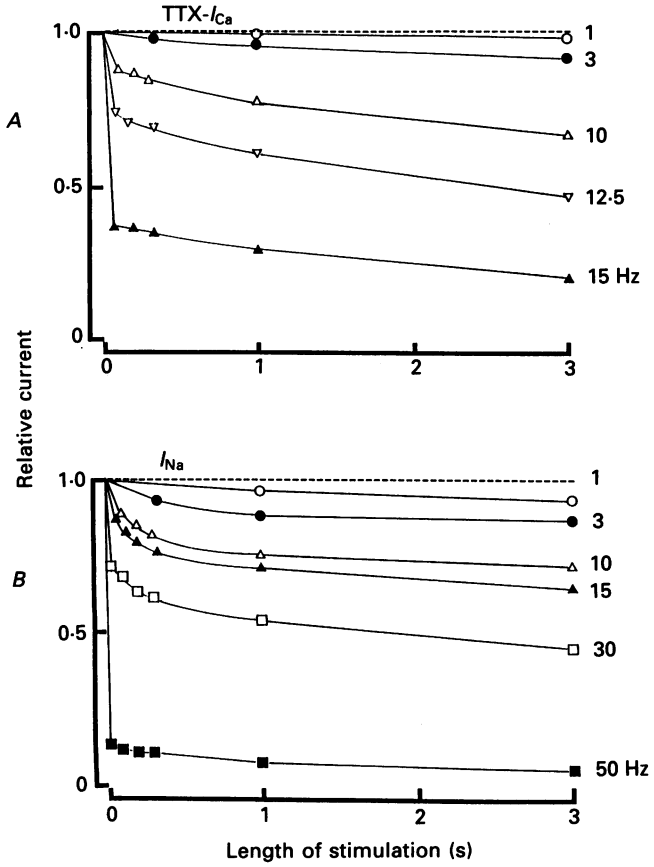

Fig. 5. Inhibition of TTX-I_{Ca} (*A*) and I_{Na} (*B*) by repetitive stimulations. Trains of depolarizing pulses from a V_h of −100 mV to −20 mV of 60 ms for TTX-I_{Ca} and 18–50 ms for I_{Na} were applied at various frequencies (1 to 50 Hz). Each point is the mean ± S.E.M. of four to six neurones.

conventional double pulse method (see inset). The recovery process of TTX-I_{Ca} as well as both I_{Na} and T-type I_{Ca} could be fitted by a double exponent. The faster component had a time constant of 13·1 ± 1·0 ms ($n = 4$) and 84·3 ± 4·2 % of recovery was through this process for TTX-I_{Ca}, 7·6 ± 1·1 ms ($n = 4$) and 89·6 ± 1·4 % for I_{Na}, and 295 ± 67 ms ($n = 6$) and 79 ± 10 % for T-type I_{Ca}, respectively. The slow component had a time constant of 120–240 ms for TTX-I_{Ca}, 80–180 ms for I_{Na}, and 4–5 s for T-type-I_{Ca}, respectively.

A train of command pulses (from a V_h of −100 to −20 mV) was applied at different pulse intervals ranging from 1 to 50 Hz. In this experiment, all neurones were left in a resting state for more than 1 min before a train of stimulation. Both

TTX-I_{Ca} and I_{Na} remained fairly constant up to each 3 Hz stimulation. When the stimulation increased more than 10 Hz, the inhibition of current amplitude appeared, and the inhibition cumulatively increased with each pulse. At 15 Hz stimulation the TTX-I_{Ca} was considerably inhibited by about 20% of the control whereas the I_{Na} was

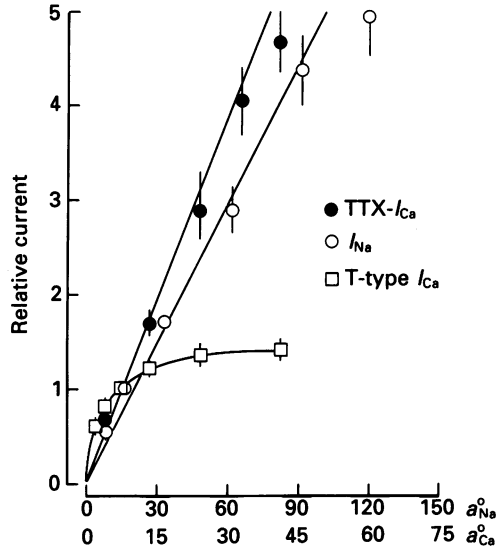

Fig. 6. Relationships between peak inward currents in the individual *I–V* relationships and $[Ca^{2+}]_o$ for both TTX-I_{Ca} (●) and T-type I_{Ca} (□) or $[Na^+]_o$ for I_{Na} (○). The values of a^o_{Na} and a^o_{Ca} on *X*-axis based on Na^+ and Ca^{2+} activities. All currents of TTX-I_{Ca} and T-type I_{Ca} were normalized to the peak response at 10 mM $[Ca^{2+}]_o$ whereas those of I_{Na} to the peak response at 20 mM $[Na^+]_o$. Both TTX-I_{Ca} and I_{Na} increased linearly with increasing a^o_{Ca} and a^o_{Na} respectively. The T-type I_{Ca} showed a hyperbolic increased as a^o_{Ca} increased (Takahashi *et al.* 1991). Each point represents the average value from five neurones and the vertical lines show means ± S.E.M.

reduced by 70% (Fig. 5) because the reactivation time of TTX-I_{Ca} was longer than that of I_{Na}, as shown in Fig. 4. In the figure the time course of the recovery (reactivation) from complete inactivation of TTX-I_{Ca} and I_{Na} was fitted by a sum of two exponential functions; i.e. the time constants of fast and slow recovery components for TTX-I_{Ca} were 13·1 ms and 120 to 240 ms and those for I_{Na} were 7·6 ms and 80 to 180 ms, respectively. Therefore, the repetitive stimulations beyond 10 Hz could inhibit the TTX-I_{Ca} more strongly than the I_{Na}. On the other hand, the amplitude of T-type I_{Ca} was suppressed by 60 and 20% of the control at 1 and 3 Hz stimulations, respectively. With the increase in the rate of stimulation, the relative strength of inhibition of current amplitude was of the order of T-type $I_{Ca} \gg$ TTX-I_{Ca} > I_{Na}. These inhibitions of TTX-I_{Ca}, I_{Na} and T-type I_{Ca} were reversed completely after the end of a train of stimulation.

Ionic dependence of the TTX-I_{Ca} and T-type I_{Ca}

To study the ionic dependence of the TTX-I_{Ca}, the amount of Ca^{2+} in the external solution was changed at the expense of choline, or Ca^{2+} was replaced by another equimolar divalent cation. When the *I–V* relationships of TTX-I_{Ca} at various

extracellular Ca^{2+} concentrations ($[Ca^{2+}]_o$) were plotted, an increase in the $[Ca^{2+}]_o$ produced an increase in the amplitude of current and also shifted the *I–V* relationships to the positive potential. Thereby, the peak inward currents in the individual *I–V* relationships were plotted as a function of $[Ca^{2+}]_o$. As seen in Fig. 6,

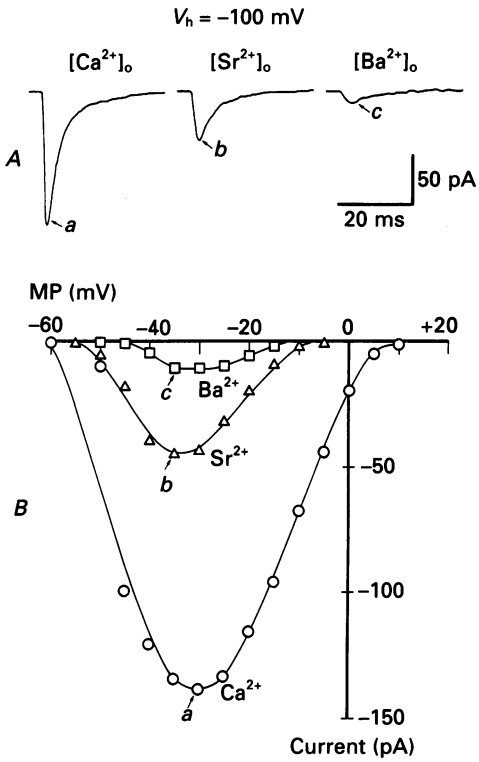

Fig. 7. Ca^{2+}, Sr^{2+} and Ba^{2+} currents in TTX-sensitive Ca^{2+} conducting channels. *A*, Ca^{2+}, Sr^{2+} and Ba^{2+} currents passing through TTX-sensitive Ca^{2+} conducting channels after substitution of external 10 mM-Ca^{2+} by equimolar Sr^{2+} or Ba^{2+}. All current recordings were obtained from the same neurone. V_h was −100 mV. Test pulse was −35 mV for TTX-I_{Ba} and TTX-I_{Sr} and −30 mV for TTX-I_{Ca}. *B*, the *I–V* relationships for TTX-sensitive I_{Ca}, I_{Sr} and I_{Ba} after the subtraction of I_{NS} are shown. The letters *a*, *b* and *c* in *A* are representative current traces at the points shown in *B*, respectively.

a linear increase of TTX-I_{Ca} with increasing $[Ca^{2+}]_o$ was observed. The amplitude of I_{Na} also increased linearly without affecting the *I–V* relationships as the external Na^+ concentration ($[Na^+]_o$) increased. In contrast, when the peak inward current of T-type I_{Ca} was plotted against $[Ca^{2+}]_o$, a clear trend towards saturation was observed, and the saturation was almost complete at around 40 mM $[Ca^{2+}]_o$ (external calcium activity $a^o_{Ca} = 24{\cdot}4$ mM). The increase of $[Ca^{2+}]_o$ also clearly shifted the *I–V* relationships of T-type I_{Ca} to the positive potential.

When 10 mM-Ca^{2+} in external solution containing 10^{-5} M-La^{3+} was replaced with Sr^{2+} or Ba^{2+}, the inward currents passing through TTX-sensitive Ca^{2+} conducting channels were reduced (Fig. 7*A*). Also, the potential of maximum inward current in individual *I–V* relationships was shifted slightly to the left in external solution

containing Sr^{2+} and Ba^{2+}, indicating the different effects of these divalent cations on the membrane surface charge (Ohmori & Yoshi, 1977). Therefore, the apparent activity sequence obtained from the maximum inward current in individual *I–V* relationships for Ca^{2+}, Sr^{2+} and Ba^{2+} currents in TTX-sensitive Ca^{2+} conducting

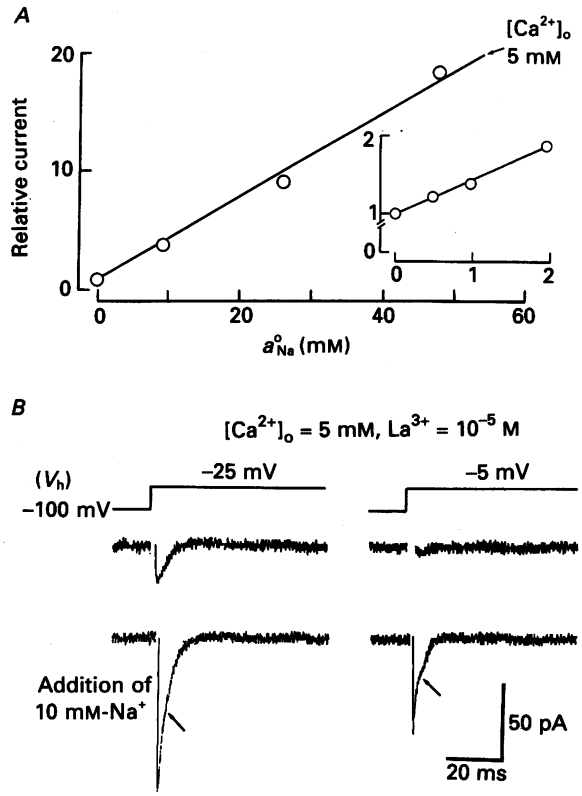

Fig. 8. Effect of $[Na^+]_o$ on TTX-I_{Ca}. All experiments were carried out in TTX-free external solution containing 10^{-5} M-La^{3+}. *A*, relationship between the relative current amplitude and a^o_{Na}. Note a linear increase of current amplitude as a^o_{Na} increased. All currents were normalized to the peak inward current evoked by depolarizing pulse from a V_h of −100 mV to −25 mV in Na^+-free external solution containing 5 mM-Ca^{2+}. Each point is the average of four to six neurones. *B*, appearance of inward current having a 'notch' in the inactivation phase by adding extracellular Na^+. Arrows show a 'notch', indicating that the inward current consists of fast and slow current components.

channels was in the order of $Ca^{2+} \gg Sr^{2+} \gg Ba^{2+}$ (Fig. 7*B*). The ratio of current amplitude was $Ca^{2+}:Sr^{2+}:Ba^{2+} = 1{\cdot}00:0{\cdot}33:0{\cdot}05$ ($n = 6$). On the other hand, as 10 mM-$CaCl_2$ in the external solution containing 10^{-7} M-TTX was replaced with equimolar $SrCl_2$ or $BaCl_2$, the relative current amplitude obtained from the maximum inward current in individual *I–V* relationships for Ca^{2+}, Sr^{2+} and Ba^{2+} currents in T-type Ca^{2+} channels was $Ca^{2+}:Sr^{2+}:Ba^{2+} = 1{\cdot}00:1{\cdot}24:0{\cdot}71$ ($n = 8$). The replacement of Ca^{2+} with Sr^{2+} or Ba^{2+} also shifted the *I–V* relationships of T-type Ca^{2+} channel to the left (Takahashi *et al.* 1991).

When the effects of extracellular Na^+ concentration $([Na^+])_o$ on TTX-I_{Ca} evoked

in external solution containing 5 mM-Ca^{2+} was examined, the inward current was enhanced linearly with increasing $[Na^+]_o$ from 0·1 to 60 mM, indicating that the TTX-I_{Ca} was not affected by adding extracellular Na^+ (Fig. 8*A*). In addition, at depolarizing step potentials beyond −25 mV, the inactivation phase of inward current in an external solution containing both 5 mM-Ca^{2+} and 10 mM-Na^+ consisted of a sum of fast and slow current components (see arrows in Fig. 8*B*), which reflected the respective inactivation kinetics of voltage-dependent Na^+ channels and TTX-sensitive Ca^{2+} conducting channels, respectively (Fig. 2*C*). Moreover, as seen in Fig. 8*B* lower panel, the amplitude of both the fast and slow current components increased with the addition of Na^+. The results suggest that Na^+ is passing through not only the voltage-dependent Na^+ channels having fast current kinetics but also the TTX-sensitive Ca^{2+} conducting channels having relative slow current kinetics.

Blockade of the TTX-I_{Ca} by TTX and lignocaine

For recording of the TTX-I_{Ca}, neurones were voltage-clamped at a V_h of −100 mV throughout the experiment. A depolarizing step of 80 mV lasting for 60 ms was applied to the preparations at 1 Hz. No use-dependent change in the amplitude of TTX-I_{Ca} was observed under this stimulus frequency (Fig. 5*A*). The TTX-I_{Ca} was sensitive to Na^+ channel blockers. The inhibitory effect of TTX on TTX-I_{Ca} developed in a concentration- and time-dependent manner without affecting the activation and inactivation processes (Fig. 9*A*). Figure 9*C* summarizes the inhibition curve of TTX on the TTX-I_{Ca}. The threshold concentration of TTX depressing the TTX-I_{Ca} was less than 10^{-9} M. With regard to the action on the maximum amplitude, a half-maximum inhibition concentration (IC_{50}) was $3{\cdot}5 \times 10^{-9}$ M and at a concentration beyond 3×10^{-8} M the TTX completely abolished the TTX-I_{Ca} in most neurones. The *I–V* relationship of TTX-I_{Ca} did not shift in the presence of TTX. The time course for reaching a steady state of the inhibitory action shortened with increasing TTX concentration, but the time courses of recovery from the inhibition after washing out the toxin were the same at different TTX concentrations, indicating that the dissociation of TTX from the binding site is independent of the TTX concentrations used.

Figure 9*B* shows the inhibitory action of lignocaine on TTX-I_{Ca}. The inhibition required only a few seconds to reach a steady-state inhibition at the concentrations used. There was no apparent difference between the time courses in the onset of inhibition and recovery from the inhibition. However, the inhibitory action of lignocaine was associated with accelerated current kinetics of both the activation and inactivation phases. Thereby, the time to peak and the half-decay time of TTX-I_{Ca} was shortened in the presence of this drug. The IC_{50} was $3{\cdot}6 \times 10^{-4}$ M (Fig. 9*C*). Lignocaine also suppressed the T-type I_{Ca}, but the inhibitory action was stronger in TTX-I_{Ca} than in T-type I_{Ca}. The IC_{50} for T-type I_{Ca} was $1{\cdot}8 \times 10^{-3}$ M (Fig. 9*C*).

Effects of T-type Ca^{2+} channel blockers on TTX-I_{Ca}

As candidates for selective and potent blockers of T-type Ca^{2+} channel compounds such as amiloride, octanol and flunarizine were reported in mouse neuroblastoma (Tang, Presser & Morad, 1988), guinea-pig brainstem slice (Llinás & Yarom, 1986),

chick sensory neurone (Fox *et al.* 1987), and rat hypothalamic neurone (Akaike *et al.* 1989). Therefore, these three compounds were tested on both TTX-I_{Ca} and T-type I_{Ca} which were evoked in 10 mM-Ca^{2+} external solution containing 10^{-5} M-La^{3+} and 10^{-7} M-TTX, respectively. The neurones were held at a V_h of -100 mV and activated

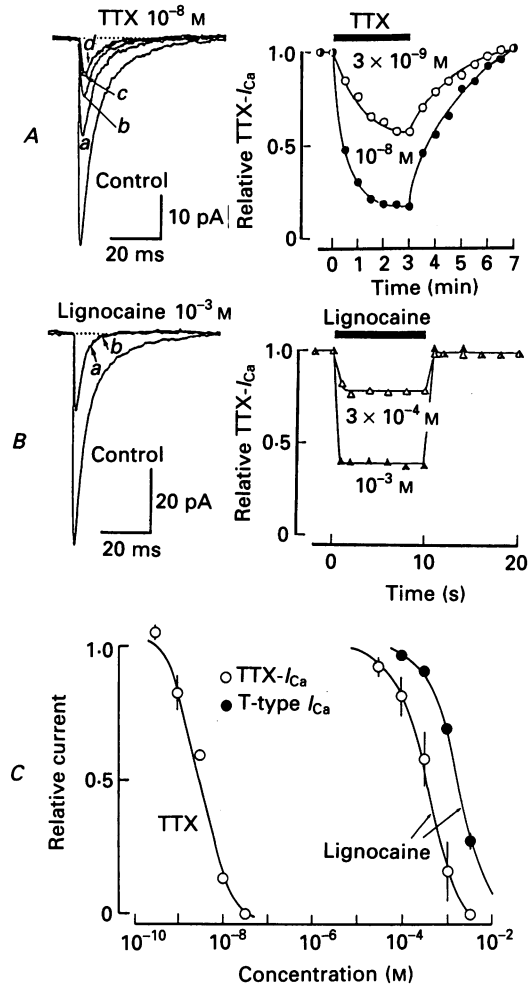

Fig. 9. Effects of TTX and lignocaine on TTX-I_{Ca}. *A* (left panel), the current traces of TTX-I_{Ca} before (control) and 0·5 (*a*), 1 (*b*), 2 (*c*) and 3 (*d*) min after the application of 10^{-8} M-TTX. The dotted line at zero current level shows the holding current level (-100 mV). *A* (right panel), the different time courses of inhibitory action of TTX at two different concentrations, and the recovery at the same time course as the inhibitions. Black bar over the lines indicates the application period of TTX. Each point is the mean value of four neurones. *B* (left panel), the currents of TTX-I_{Ca} before (control) and 1 (*a*) and 10 (*b*) s after the application of 10^{-3} M-lignocaine. *B* (right panel), the concentration-dependent inhibition of lignocaine at two concentrations and the recovery from the inhibition. Note the time scale in second order. Each point shows the mean value of four experiments. *C*, the inhibitory actions of TTX and lignocaine on the peak amplitude of TTX-I_{Ca} (○). The lignocaine action was also tested on T-type I_{Ca} (●). Each point is the mean ± S.E.M. of four experiments.

by a step depolarization to −30 mV at every 30 s with or without the blockers. As shown in Fig. 10, amiloride had no effect on TTX-I_{Ca} (data not shown) but suppressed the T-type I_{Ca}. The inhibitory effect of octanol was stronger on TTX-I_{Ca} ($IC_{50} = 1{\cdot}7 \times 10^{-4}$ M) than on T-type I_{Ca} ($IC_{50} = 2{\cdot}8 \times 10^{-4}$ M). Flunarizine suppressed

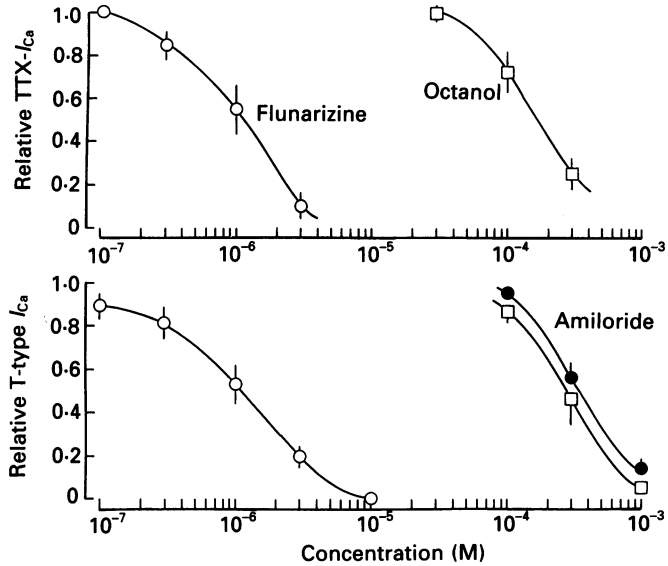

Fig. 10. Effects of T-type Ca^{2+} channel blockers on TTX-I_{Ca} (upper panel) and T-type I_{Ca} (lower panel). All currents were evoked by a depolarized pulse to −30 mV from a V_h of −100 mV at every 30 s. Each point is the average of four to six neurones. Vertical bars show ± S.E.M.

equally the TTX-I_{Ca} ($IC_{50} = 1{\cdot}2 \times 10^{-6}$ M) and T-type I_{Ca} ($IC_{50} = 1{\cdot}0 \times 10^{-6}$ M). The kinetics of both currents were not affected by these drugs at concentrations used.

Effect of scorpion toxin on TTX-I_{Ca}

Neurones were voltage-clamped at a V_h of −100 mV and depolarizing pulses of 60 ms in duration were applied to elicite the TTX-I_{Ca}. The peak inward current was recorded at the membrane potential of −30 mV. The toxin (1 μg ml^{-1}) prolonged the inactivation phase of TTX-I_{Ca}. The effect on the current inactivation was complete within 3 to 5 min after adding the toxin. The semilogarithmic plots of the inactivation phase of TTX-I_{Ca} could be fitted with fast and slow exponential components (τ_{if} and τ_{is}, respectively) before (control) and 3 min after adding the toxin. When the amplitudes of fast and slow current components were estimated from the semilogarithmic plots (curve fitting) of the inactivation process of the TTX-I_{Ca}, the scorpion toxin increased the fractional contribution of the slow current component to the total current amplitude whereas the contribution of the fast one decreased. The toxin had the same effect on I_{Na} in this preparation (Kaneda, Oyama, Ikemoto & Akaike, 1989). However, the scorpion toxin (1 mg ml^{-1}) did not affect the T-type I_{Ca}.

DISCUSSION

We have demonstrated distinct voltage dependence, kinetics, ionic selectivity and pharmacological characteristics of the TTX-sensitive Ca^{2+} conducting channels in the pyramidal neurones freshly dissociated from the rat hippocampal CA1 region. The kinetic properties of TTX-I_{Ca} were very similar to those of I_{Na}, and the TTX-I_{Ca} was unique in its high sensitivity to Na^+ channel modulators such as TTX, lignocaine and scorpion toxin. The following results suggest that the TTX-I_{Ca} is passing through the Ca^{2+} conducting Na^+ channels. (1) The transient TTX-I_{Ca} and I_{Na} activated at potentials above -60 mV and reached their current peaks at about -30 mV in a highly potential-dependent manner. The potentials of full activation were -30 mV for TTX-I_{Ca} and -20 mV for I_{Na}. The inactivation processes of both TTX-I_{Ca} and I_{Na} were fitted by a sum of two exponential functions while that of T-type I_{Ca} was fitted by a single exponential function (Akaike *et al.* 1989). The midpotentials in the steady-state inactivation curves of TTX-I_{Ca}, I_{Na} and T-type I_{Ca} were $-72{\cdot}5$, $-74{\cdot}5$ and -79 mV, respectively. (2) The ratio of time constant of the major component of recovery from the complete inactivation of TTX-I_{Ca}, I_{Na} and T-type I_{Ca} was in the order of 1 : 0·6 : 23. (3) The order of frequency-dependent inhibition was T-type $I_{Ca} \gg$ TTX-$I_{Ca} > I_{Na}$. (4) When the peak amplitudes in the I–V relationship of TTX-I_{Ca} and I_{Na} were plotted as a function of $[Ca^{2+}]_o$ and $[Na^+]_o$, the current amplitudes increased linearly with increasing $[Ca^{2+}]_o$ and $[Na^+]_o$, respectively. On the other hand, the T-type I_{Ca} increased in a hyperbolic manner as $[Ca^{2+}]_o$ increased. (5) The Na^+ channel of hippocampal pyramidal neurones was highly sensitive to TTX which suppressed the current in a concentration- and time-dependent fashion without affecting the current kinetics (Kaneda *et al.* 1989). They also reported that lignocaine reduced I_{Na} in a concentration-dependent manner with accelerating current kinetics, indicating the blockade of the open state of the Na^+ channels (Yeh & Narahashi, 1977). The IC_{50} values of TTX and lignocaine on I_{Na} were 10^{-8} M and 4×10^{-4} M, respectively. In the present experiment, the IC_{50} values of TTX and lignocaine on TTX-I_{Ca} were $3{\cdot}5 \times 10^{-9}$ M and $3{\cdot}6 \times 10^{-4}$ M, respectively. No difference in the inhibitory actions of TTX and lignocaine on both TTX-I_{Ca} and I_{Na} was observed. The TTX-I_{Ca} was insensitive to an inorganic Ca^{2+} blocker, La^{3+} at 10^{-5} M, at which concentration T-, N- and L-type Ca^{2+} channels were completely blocked (Takahashi *et al.* 1989). (6) The action of scorpion toxin on the inactivation process of TTX-I_{Ca} was essentially similar to that of I_{Na} in the frog node of Ranvier (Mozhayeva, Naumov, Nosyreva & Grishin, 1980; Benoit & Dubois, 1987), squid axonal membrane (Narahashi, Shapiro, Deguchi, Scuka & Wang, 1972), and rat hippocampal pyramidal neurone (Kaneda *et al.* 1989). (7) The current amplitude of TTX-I_{Ca} was increased by adding Na^+ extracellularly (see Fig. 8), indicating Na^+ can also pass through these TTX-sensitive Ca^{2+} conducting channels.

When the hippocampal pyramidal neurones were superfused with external solution containing 10 mM-Ca^{2+}, Sr^{2+} or Ba^{2+}, the ionic selectivity of the TTX-sensitive Ca^{2+} conducting channels for these divalent cations was in the order of $Ca^{2+} \gg Sr^{2+} > Ba^{2+}$ (Fig. 7). The selectivity differed markedly from the order ($Sr^{2+} \gg Ca^{2+} > Ba^{2+}$) of T-type Ca^{2+} channels in the same hippocampal preparation (Takahashi *et al.* 1991), in rat hypothalamic neurones (Akaike *et al.* 1989) and cultured

hippocampal neurone from fetal rat (Yaari, Hamon & Lux, 1987). A similar ionic selectivity among Ca^{2+}, Sr^{2+} and Ba^{2+}, being $Ca^{2+} \gg Sr^{2+} > Ba^{2+} = 0$, was observed for the '$Ca^{2+}$ current' through 'Na^+ channels' having faster current kinetics than the 'Ca^{2+} current' through 'Ca^{2+} channels' in egg cell membrane of the tunicate (Okamoto *et al.* 1976).

In CNS neurones the T-type Ca^{2+} channels play an important role in functions by contributing to spontaneous depolarization waves as a generator of pacemaker activity and a rebound excitation (Llinás & Yarom, 1981; Choi, 1988). The TTX-I_{Ca} and T-type I_{Ca} heterogeneously distributed in the dorsal and ventral sites of rat hippocampal CA1 region, and the amplitude of TTX-I_{Ca} in the dorsal portion is almost equal to that of T-type I_{Ca} in the ventral portion (Akaike *et al.* 1991). Both currents were activated around -60 mV at near resting potential. In addition, the half-recovery time from the complete inactivation of TTX-I_{Ca} was about 20 to 30 times more rapid than that of T-type I_{Ca} (Fig. 4). Concerning the possible role of the TTX-I_{Ca} in the hippocampal pyramidal neurones, therefore, the results suggest that the TTX-I_{Ca} may act like I_{Na} and contribute more effectively to spontaneous depolarization waves and bursting activities of the pyramidal neurones than does T-type I_{Ca}.

This study was supported by Grants-in-Aid for Scientific Research (No. 02404022) to N. Akaike from the Ministry of Education, Science and Culture, Japan.

REFERENCES

AKAIKE, N., INOUE, M. & KRISHTAL, O. A. (1986). 'Concentration clamp' study of γ-aminobutyric acid-induced chloride current kinetics in frog sensory neurones. *Journal of Physiology* **379**, 171–185.

AKAIKE, N., KOSTYUK, P. G. & OSIPCHUK, Y. V. (1989). Dihydropyridine-sensitive low-threshold calcium channels in isolated rat hypothalamic neurones. *Journal of Physiology* **412**, 181–195.

AKAIKE, N., TAKAHASHI, K. & MORIMOTO, M. (1991). Heterogeneous distribution of tetrodotoxin-sensitive calcium-conducting channels in rat hippocampal CA1 neurons. *Brain Research* **556**, 135–138.

BARKER, P. F., HODGKIN, A. L. & RIDGWAY, E. B. (1971). Depolarization and calcium entry in squid giant axons. *Journal of Physiology* **218**, 709–755.

BENOIT, E. & DUBOIS, J. (1987). Properties of maintained sodium current induced by a toxin from *Androctonus* scorpion in frog node of Ranvier. *Journal of Physiology* **383**, 93–114.

CHOI, D. W. (1988). Calcium-mediated neurotoxicity: Relationship to specific channel types and role in ischemic damage. *Trends in Neurosciences* **1**, 465–469.

FOX, A. P., NOWYCKY, M. C. & TSIEN, R. (1987). Kinetic and pharmacological properties distinguishing three types of calcium currents in chick sensory neurones. *Journal of Physiology* **394**, 149–172.

HODGKIN, A. L. & KEYNES, R. D. (1957). Movements of labelled calcium in squid giant axons. *Journal of Physiology* **138**, 253–281.

KANEDA, M., NAKAMURA, H. & AKAIKE, N. (1988). Mechanical and enzymatic isolation of mammalian CNS neurones. *Neuroscience Research* **5**, 299–315.

KANEDA, M., OYAMA, Y., IKEMOTO, Y. & AKAIKE, N. (1989). Scorpion toxin prolongs an inactivation phase of the voltage-dependent sodium current in rat isolated single hippocampal neurons. *Brain Research* **487**, 192–195.

LLINÁS, R. & YAROM, Y. (1981). Electrophysiology of mammalian inferior olivary neurones *in vitro*. Different types of voltage-dependent ionic conductances. *Journal of Physiology* **315**, 549–567.

LLINÁS, R. & YAROM, Y. (1986). Specific blockade of the low threshold calcium channel by high molecular weight alcohols. *Society for Neuroscience Abstracts* 174.

MEVES, H. & VOGEL, W. (1973). Calcium inward currents in internally perfused giant axons. *Journal of Physiology* **235**, 225–265.

MOZHAYEVA, G. N., NAUMOV, A. P., NOSYREVA, E. D. & GRISHIN, E. V. (1980). Potential-dependent interaction of toxin venom of the scorpion *Buthus eupeus* with sodium channels in myelinated fibre. *Biochimica et Biophysica Acta* **597**, 587–602.

NARAHASHI, T., SHAPIRO, B. I., DEGUCHI, T., SCUKA, M. & WANG, C. M. (1972). Effects of scorpion venom on squid axon membranes. *American Journal of Physiology* **222**, 850–857.

OHMORI, H. & YOSHII, M. (1977). Surface potential reflected in both gating and permeation mehanisms of sodium and calcium channels of the tunicate egg cell membrane. *Journal of Physiology* **267**, 429–463.

OKAMOTO, H., TAKAHASHI, K. & YOSHII, M. (1975). Membrane currents of the tunicate egg under the voltage clamp condition. *Journal of Physiology* **254**, 607–638.

OKAMOTO, H., TAKAHASHI, K. & YOSHII, M. (1976). Two components of the calcium current in the egg cell membrane of the tunicate. *Journal of Physiology* **255**, 527–561.

SORBERA, L. A. & MORAD, M. (1990). Atrionatriuretic peptide transforms cardiac sodium channels into calcium-conducting channels. *Science* **247**, 969–973.

TAKAHASHI, K., UENO, S. & AKAIKE, N. (1991). Kinetic properties of T-type Ca^{2+} currents in isolated rat hippocampal CA1 pyramidal neurons. *Journal of Neurophysiology* **65**, 148–155.

TAKAHASHI, K., WAKAMORI, M. & AKAIKE, N. (1989). Hippocampal CA1 pyramidal cells of rats have four voltage-dependent calcium conductances. *Neuroscience Letters* **104**, 229–234.

TANG, C. M., PRESSER, F. & MORAD, M. (1988). Amiloride selectively blocks the low threshold (T) calcium channel. *Science* **240**, 213–215.

TSAKI, I., WATANABE, A. & LERMAN, L. (1967). Role of divalent cations in excitation of squid giant axons. *American Journal of Physiology* **213**, 1465–1474.

WATANABE, A., TASAKI, I., SINGER, I. & LERMAN, L. (1967). Effect of tetrodotoxin on excitability of squid giant axons in sodium free media. *Science* **158**, 95–97.

YARRI, Y., HAMON, B. & LUX, H. D. (1987). Development of two types of calcium channels in cultured mammalian hippocampal neurons. *Science* **235**, 680–682.

YEH, J. Z. & NARAHASHI, T. (1977). Kinetic analysis of pancuronium interaction with sodium channels in squid axon membranes. *Journal of General Physiology* **69**, 293–323.